Journal of Ceramic Processing Research. Vol. 16, No. 5, pp. 525~530 (2015)

J O U R N A L O F
Ceramic Processing Research

Crystallization Behavior of Sm^{3+} doped $Ba_2TiSi_2O_8$ Glass Prepared by Containerless Aerodynamic Levitation Technology

Sang-Kyo Jung[a], Chi-Hoon Lee[a], Chi-Hwan Lee[a] and Won-Seung Cho[a,*]
School of Materials Science and Engineering, Inha University, 253 Yonghyun-Dong, Nam-Gu, Incheon 402-751, Korea

Spherical Sm^{3+} doped $Ba_2TiSi_2O_8$ (BTS) glasses were prepared using containerless aerodynamic levitation technology. The glass prepared by aerodynamic levitation technology exhibited enhanced glass stability compared to the conventional glass-making process via melt-quenching. With increasing heat treatment temperature, the lattice parameter (a) of the nano- or micro-crystalline BTS crystals formed in the glass decreased, but the lattice parameter (c) increased. The values of the Avrami exponent (n) and Ozawa exponent (m) for Sm^{3+} doped BTS glass calculated using the Ozawa equation and Mo equation were both approximately 3, indicating the three-dimensional growth of BTS crystals. The activation energies using the modified Ozawa equation and modified Kissinger equation were 530.3 kJ/mol and 524.3 kJ/mol, respectively. Nanocrystallized Sm^{3+} doped BTS glass exhibited yellow-green (564 nm), orange (601 nm) and red (647 and 709 nm) luminescence. The optimal heat treatment for high efficiency PL emission was found to be 750 °C.

Key words: Aerodynamic levitation, $Ba_2TiSi_2O_8$, Microstructure, Crystallization parameter, Photoluminescence.

Introduction

Nanostructures are the gate-way to a new realm in physical, chemical, biological, and materials science. The crystallization of glass is an effective method for fabricating nanostructures [1]. Recently, new optically transparent bulk nanocrystallized glasses (so-called glass-ceramics) were fabricated successfully in some glasses [2-5]. Among them, transparent nanocrystallized glasses consisting of nonlinear optical/ferroelectric nanocrystals have attracted considerable attention because of their potential applications in photonic devices, such as tunable waveguides and optical switching [6, 7].

Fresnoite (BTS; $Ba_2TiSi_2O_8$) exhibit blue-white luminescence with no activator [8] as well as non-linear optical properties [9]. The photoluminescence (PL) of rare-earth (RE) ions in glassy or crystalline solids has been used for a range of photonic devices. Zhu *et al.* [10] examined the upconversion luminescence properties of the Sm^{3+} doped BTS glass and glass-ceramics. On the other hand, glass with a stoichiometric BTS composition exhibited an extremely high nucleation rate ($\sim 10^{17}\ m^{-3}\ s^{-1}$) [11] and an extremely high tendency of phase separation. The interface of phase separation is thermodynamically unstable. Because the interface can act as a nucleation site, conventional melted BTS glass would have an extremely high nucleation rate [12].

Recently, containerless levitation techniques were developed to avoid chemical contamination and heterogeneous nucleation at the container wall. In particular, these processes enable the liquid to deeply supercool at a relatively low cooling rate [13, 14]. Levitation techniques can be used to develop amorphous phases with novel functional properties. The typical levitation technologies are acoustic, electromagnetic, electrostatic, aerodynamic levitation, etc. Among them, aerodynamic levitation technology is used mainly to study ceramic materials and has economic merits [15, 16].

On the other hand, knowledge of the nucleation and crystallization kinetic parameters, such as the activation energy for crystal growth and crystal growth mechanism, is important for the preparation of glass-ceramics with the desired microstructure and properties [17].

Therefore, in this study, spherical BTS and Sm^{3+} doped BTS glasses were prepared by aerodynamic levitation. The effects of the heat-treatment temperature on the microstructure were investigated to determine the crystallization behavior in the as-levitated glass. The as-levitated Sm^{3+} doped BTS glasses were analyzed by differential scanning calorimetry (DSC) to investigate the crystallization kinetic parameters. Finally, the optical properties, such as photoluminescence and refractive index, were investigated.

Experimental Procedures

sample preparation

The glass composition of $40BaO\text{-}20TiO_2\text{-}40SiO_2\text{-}0.5Sm_2O_3$ (mol%) was prepared. As raw materials,

*Corresponding author:
Tel : +82-32-860-7528
Fax: +82-32-862-5546
E-mail: wscho@inha.ac.kr

$BaCO_3$ (practical grade, Duksan Pure Chemical, Co., LTD., Korea), TiO_2 (99.9%, High Purity Chemicals Co., LTD., Japan), SiO_2 (99.99%, High Purity Chemicals Co., LTD., Japan), and Sm_2O_3 (99.9%, Shin-Etsu Chemical Co., LTD., Japan) were used. The powders at the required stoichiometry were ball-milled for 24 h in an ethanol medium using a plastic jar with ZrO_2 balls. The slurries were dried simultaneously using a rotary evaporator. The glass batch was poured into a Pt crucible (50 ml) and kept at 800 °C for 30 min to remove the CO_2 due to the decomposition of $BaCO_3$ ($BaCO_3(s)BaO(s) + CO_2(g)$). Finally, the glass batch was melted at 1550 °C for 1 h. For vitrification, the melt was poured onto a graphite plate kept at 20 °C, and quenched by pressing the stainless steel.

A spherical sample, 2.5 mm in diameter, was levitated using an aerodynamic levitator with O_2 gas at a flow rate of 416 ml/min. Details of the levitation experiment are reported elsewhere [18].

Property measurement

The samples were crushed and ground using an agate mortar and pestle. The powdered material was used for differential scanning calorimetry (DSC) and x-ray diffraction (XRD). The glass transition and crystallization temperatures of the as-levitated sample were estimated by DSC (404 F1, NETZSCH). In the DSC experiment, the powdered samples were placed into a Pt crucible and heated from room temperature to 1450 °C at a heating rate of 10 °C/min in air.

Sm^{3+} doped BTS glasses were heat treated for 1 h in air at temperatures ranging from the glass transition temperature to the crystallization onset temperature. Hereafter, the Sm^{3+} doped BTS is called Sm-BTS. The heat treatment temperature range for the levitated Sm-BTS glasses was 730 °C-770 °C. The crystalline structure of the samples was analyzed by XRD (DMAX-2500, Rigaku) using Cu Kα radiation in the 2θ range, 10 °-90 ° 2θ, at a scanning rate of 0.5 °/min. The crystallinity of Sm-BTS glass ceramics as a function of the heat treatment temperature was calculated from the XRD peaks by the ratio of the sum of the areas under all the crystalline peaks to the sum of the areas under the crystalline and amorphous peaks. The lattice parameters (a and c) of the BTS phase (tetragonal structure) were calculated from the XRD patterns using the Nelson-Riley extrapolation [19]. DSC analyses of the levitated Sm-BTS were carried out at five different heating rates (3, 6, 9, 12, and 15 °C/min) to examine the crystallization kinetic parameters. The photoluminescence (PL) of the samples was measured at room temperature using PL spectrometer (SPEX 1403, SPEX). A He-Cd laser (55 mW) with a wavelength of 325 nm as the excitation source. Finally, the refractive indices were measured by spectroscopic ellipsometry at 587.6 nm.

Results and Discussion

Fig. 1 presents the typical cooling curve for the Sm-BTS molten droplet (glass) during levitation. The Sm-BTS glass was kept at 1766 °C (> melting point (1424 °C) of Sm-BTS) for 30 seconds and then cooled. The sample was cooled continuously to ambient temperature without showing recalescence. This was reconfirmed by snap shot images showing the Sm-BTS molten droplet during the cooling stage. The cooling rate over temperature range from 1766 °C to 1000 °C was 324 °C/s.

An almost spherical Sm-BTS glass with a diameter of 2.5 mm was fabricated. The appearance of the levitated sample was transparent, indicating an amorphous phase. As mentioned above, the levitation process can prevent heterogeneous nucleation during solidification and provide a relatively rapid cooling rate, thereby enhancing vitrification.

Fig. 2 shows the results of DSC analyses for the conventional melt-quenched and levitated Sm-BTS glasses. From the DSC curves, the glass transition (T_g), crystallization onset (T_x), crystallization peak (T_p), and melting temperatures (T_m) were determined. The values of T_g, T_x, T_p, and T_m for the levitated Sm-BTS glass were 714 °C, 797 °C, 814 °C, and 1424 °C, respectively. The corresponding values for the conventional melt-quenched Sm-BTS glass were 709 °C, 783 °C, 809 °C, and 1424 °C. In the case of the levitated Sm-BTS glass, T_g, T_x and T_p, increased slightly compared to the conventional melt-quenched Sm-BTS glass. This indicates improved glass stability in the levitated glass.

Hrubý suggested that the parameter, K_H, obtained by differential thermal analysis (DTA) or DSC, indicates the glass stability against crystallization upon heating [20]. According to Hrubý, a higher K_H value of a certain glass indicates higher stability against crystallization upon heating, and presumably, higher vitrification ability upon cooling [20]. In this study, K_H values for the conventional

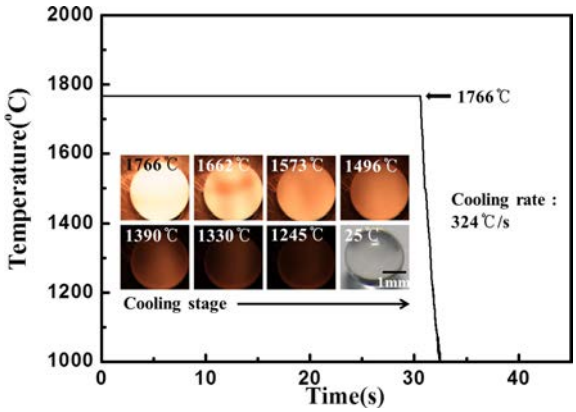

Fig. 1. Typical cooling curve for Sm^{3+} doped BTS glass during aerodynamic levitation. The insets in the figure show snap shot images of molten droplets and solidified glass. The images were taken using a high speed video camera during the cooling stage.

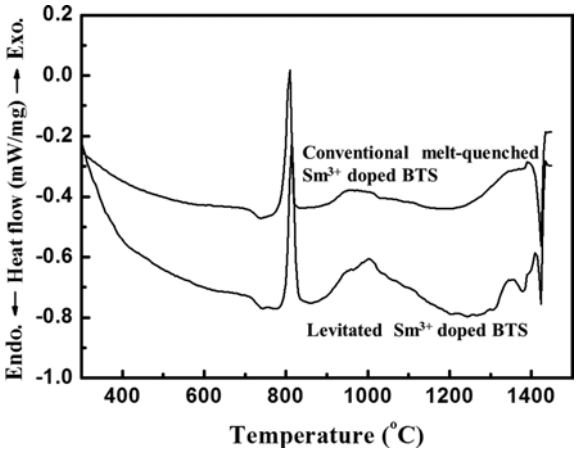

Fig. 2. DSC analyses of conventional melt-quenched Sm^{3+} doped BTS and levitated Sm^{3+} doped BTS glasses.

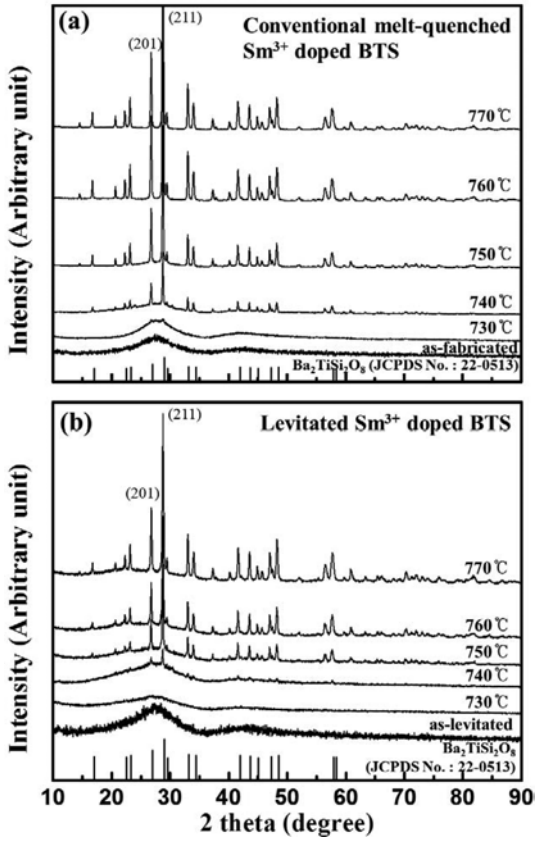

Fig. 3. XRD patterns for levitated (a) conventional melt-quenched Sm^{3+} doped BTS and (b) levitated Sm^{3+} doped BTS glasses. Each sample was heated at the desired temperature for 1 h prior to XRD analysis.

melt-quenched Sm-BTS glass and levitated Sm-BTS glass were 0.12 and 0.13, respectively. As the typical K_H values of glass range between 0.1 and 2 [20], K_H = 0.12-0.13, indicates a higher tendency of Sm-BTS glass to crystallize than typical glasses, as reported elsewhere [11].

Fig. 3 shows the XRD patterns for (a) conventional melt-quenched Sm-BTS and (b) levitated Sm-BTS glasses as a function of the heat treatment temperature.

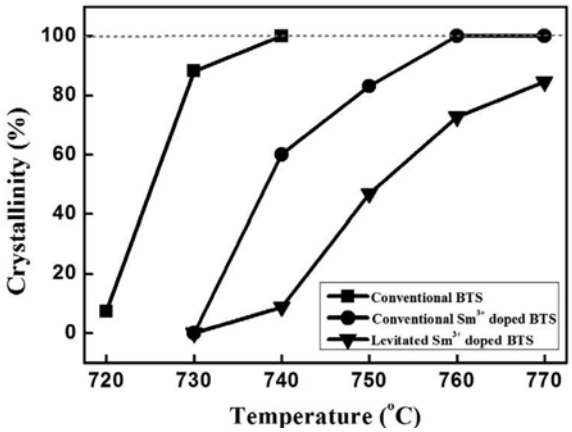

Fig. 4. Degree of crystallization of BTS and Sm^{3+} doped BTS glass-ceramics as a function of the heat treatment temperature. The glasses were prepared by an aerodynamic levitation and conventional glass-making process. The glasses were held for 1 h at each temperature prior to XRD analysis.

Broad humps were observed at ~ 27° 2θ in both the as-levitated sample and the samples heat-treated at 730 ºC-740 ºC, indicating the presence of amorphous phases. The tiny peaks corresponding to the (201) and (211) planes, which are main peaks of BTS, appeared after heat-treating (730 ºC for the conventional melt-quenched Sm-BTS glass and 740 ºC for the Sm-BTS glass), suggesting the presence of very poorly developed micro- or nano-crystalline phases. All the peaks corresponding to BTS were detected at high temperatures (≥ 740 ºC for the melt quenched Sm-BTS glass, 750 ºC for the levitated Sm-BTS glass). Crystallization occurred at temperatures more than T_g (709 ºC for BTS glass and 714 ºC for Sm-BTS glass). The small amount of amorphous phase still remained, even after heat treatment at 750 ºC. Therefore, the percentage crystallinity of the Sm-BTS glass ceramics was calculated by comparing the areas under all the crystalline peaks and the amorphous peak.

Fig. 4 shows the percentage crystallinity of the Sm-BTS glass ceramics as a function of the heat treatment temperature. The crystallinity increased with increasing heat treatment temperature. The samples prepared using the conventional melt-quenching process were also indicated for comparison. The conventional melt-quenched BTS and Sm-BTS glasses crystallized rapidly with increasing temperature, and crystallized fully at 740 ºC and 760 ºC, respectively. The crystallization temperature of the levitated samples was shifted to a higher temperature than those in the conventionally melt-quenched glasses.

The glass with the stoichiometric BTS composition indicated an extremely high tendency of phase separation [12]. As the interface of phase separation can act as a nucleation site, the conventionally melted BTS glass would represent a high nucleation rate. On the other hand, the number of nucleation sites decreased considerably when the glass solidified rapidly during the

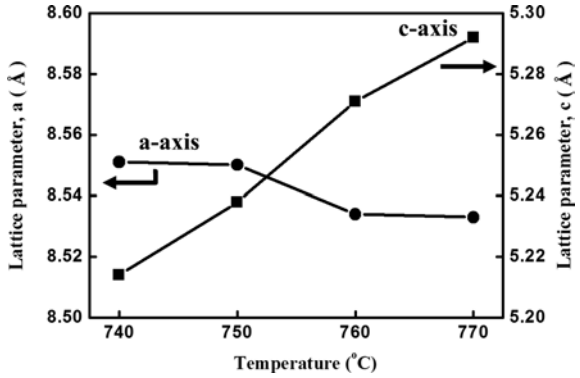

Fig. 5. Lattice parameters (a and c) of Sm^{3+} doped BTS crystals (tetragonal structure). BTS crystals were crystallized from levitated glasses by heat treatment at the desired temperature for 1 h.

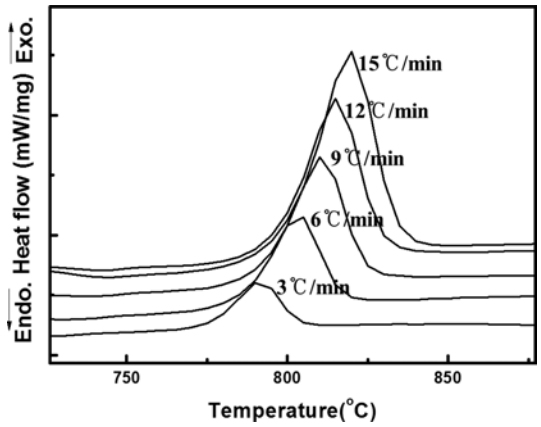

Fig. 6. DSC analyses at five different heating rates, (α = 3, 6, 9, 12, and 15 °C/min) for levitated Sm^{3+} doped BTS glasses.

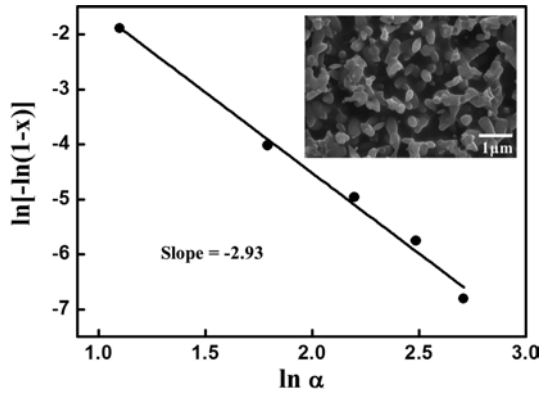

Fig. 7. Ozawa plot of ln[-ln(1-x)] vs. ln α. Microstructure of crystallized Sm^{3+} doped BTS glass was inserted in the figure, indicating three-dimentional crystal growth.

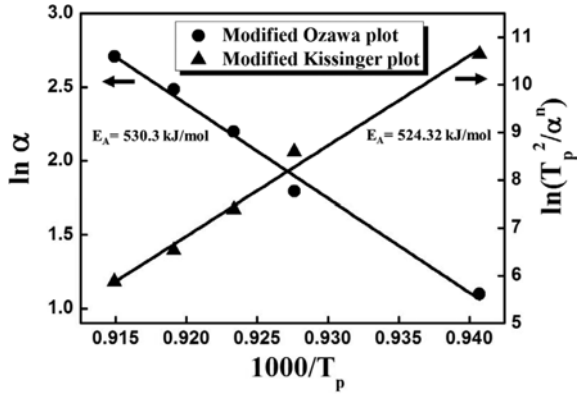

Fig. 8. Modified Ozawa plot of ln α vs. $1000/T_P$ and the modified Kissinger plot of $\ln(T_p^2/\alpha^n)$ vs. $1000/T_P$.

levitation process, resulting decreased crystallization upon subsequent heat treatment. This can explain the low tendency of crystallization in the levitated samples at a given temperature. Therefore, the levitated glass sample is expected to be easier than the conventionally melted glass samples for controlling the volume and size of the micro- or nano-crystalline BTS phase in amorphous glass.

Fig. 5 presents the lattice parameters of the levitated Sm-BTS glasses after heat-treatment for 1 h at the desired temperature. Sm^{3+} ions substitute for the Ba^{2+} sites in $Ba_2TiSi_2O_8$ nanocrystals. (Ionic radius: 0.143 nm for Ba^{2+} and 0.113 nm for Sm^{3+} [21]). With increasing heat treatment temperature, the a-axis lattice parameters (a) decreased, whereas the c-axis lattice parameters (c) increased. This was attributed to crystallization-induced stress formed in the crystallization process. Ochi [22] reported that the difference in density between the parent glass (4.05 g/cm^3) and the fresnoite crystal (4.43 g/cm^3) contributes to the crystallization-induced stress. Ochi argued that the residual stress resulting from the crystallization process applies a compression force to the layers composed of TiO_5 square pyramids and SiO_2 tetrahedra in the direction normal to the c-axis, hence the layers expand in the direction of the c-axis.

DSC analysis is carried out non-isothermally to determine the crystallization kinetic data such as the activation energy (E_A), Avrami exponent (n) and Ozawa exponent (m).

Fig. 6 shows the DSC traces at five different heating rates, (α = 3, 6, 9, 12, and 15 °C/min) for the levitated Sm-BTS glasses. The crystallization peak temperature was shifted to higher temperature with increasing heating rates. The Ozawa plot is the equation most commonly used to calculate n. Therefore, the value of the Avrami exponent (n) was determined using following Ozawa equation [23].

$$\ln[-\ln(1-x)] = -n\ln\alpha + \text{const} \quad (1)$$

where x is the crystallized fraction at temperature for a heating rate of α and n is the Avrami exponent. Therefore, a plot of ln[-ln(1-x)] vs. ln α gives a straight line with a slope of –n. The value of n was calculated from linear fits to the plot of ln[-ln(1-x)] vs. ln α, as shown in Fig. 7. The slope has a value of –2.93. Therefore, value of n is approximately 3. The inset in figure shows the microstructure of the Sm-BTS glass ceramics. Sm-BTS was crystallized at 740 °C for 1 h,

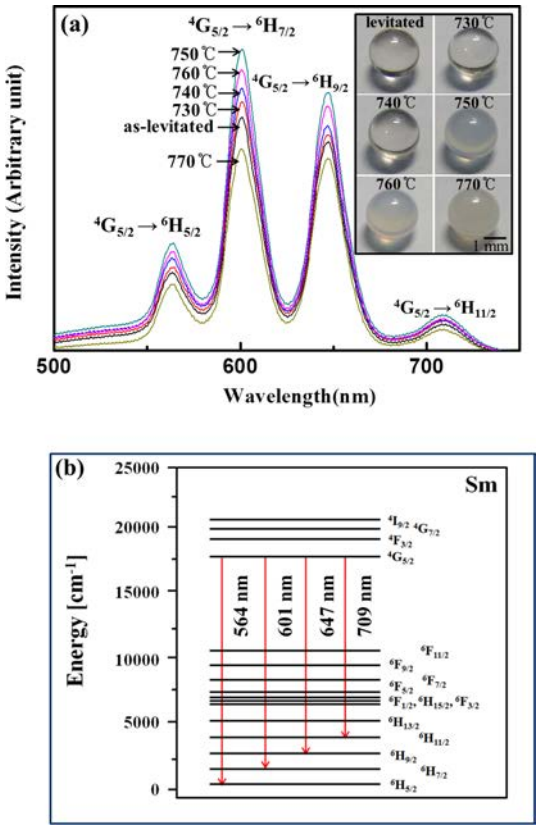

Fig. 9. Photoluminescence spectra of the levitated Sm^{3+} doped BTS glass and glass-ceramics as a function of the heat-treatment temperature. The inset shows the changes in optical transparency of glass samples with the heat-treatment temperature for 1 h. The optical transparency of levitated sample changes from transparent to translucent at temperatures higher than 750 °C.

and then etched chemically for 120 seconds at room-temperature using a mixed solution of 0.8% HF + 0.2% HCl. The microstructure of Sm-BTS revealed almost spherical-shaped crystals, indicating the three-dimensional growth of the crystals. According to the crystallization mechanism [24], n = m when the number of nuclei is fixed during crystallization and n = m + 1when the number of nuclei increased with decreasing heating rate. Three-dimensional growth corresponded to m = 3. The same values of n and m (n = m = 3) were determined for Sm-BTS glass, indicating that the number of nuclei for the levitated Sm-BTS was not changed by the heating rate.

Matusita *et al*. [25] reported that the activation energy could be calculated independently using the modified Ozawa equation or modified Kissinger equation. First, the activation energy was estimated using the modified Ozawa equation.

$$\ln\alpha = -\frac{mE_A}{nRT} - \frac{1}{n}\ln[-\ln(1-x)] + \text{const} \qquad (2)$$

where E is the activation energy for crystal growth and R is the gas constant. The activation energy was calculated from the slope of ln α vs. 1/T. As shown in Fig. 8, the slope of a plot of ln α vs. $1000/T_P$ shows a value of $-\frac{mE_A}{nR}$. The activation energy was calculated to be 530.3 kJ/mol (slope = 63.8, n = m = 3).

For comparison, the activation energy was also calculated using the modified Kissinger equation.

$$\ln\left(\frac{T_p^2}{\alpha^n}\right) = \frac{mE_A}{RT_p} + \text{const} \qquad (3)$$

where T_p is the crystallization peak temperature at a given heating rate α. E_A is the activation energy, R is the gas constant, n is the Avrami parameter and m is the numerical factor of the crystallization mechanism.

The activation energy was calculated from the slopes of a linear plot of $\ln(T_p^2/\alpha^n)$ vs. 1/T, as shown in Fig. 8. The slope of $\ln(T_p^2/\alpha^n)$ vs. $1000/T_P$ showed the value of $\frac{mE_A}{nR}$. The activation energy was calculated to be 524.3 kJ/mol (slope = 189.2, m = 3). This value is similar to the value calculated using the Ozawa equation. This result is consistent with Rangarajan et al. [26], who obtained a value of 528 kJ/mol from differential thermal analysis (DTA).

Fig. 10 shows the PL spectra of the Sm-BTS glass and crystallized glasses prepared by the levitation process. Four peaks assigned to the f-f transitions of $^4G_{5/2} \rightarrow {}^6H_{5/2}$ (yellow-green: 564 nm), $^4G_{5/2} \rightarrow {}^6H_{7/2}$ (orange: 601 nm), $^4G_{5/2} \rightarrow {}^6H_{9/2}$ (red: 647 nm), and $^4G_{5/2} \rightarrow {}^6H_{11/2}$ (red: 709 nm) were observed. This is consistent with the work by Zhu *et al*. [10]. The intensity of these peaks increased due to crystallization up to 750 ºC for 1 h, and then decreased with increasing heat treatment temperature. The inset in the figure shows the changes in the transparency of the Sm-BTS levitation sample with the heat treatment temperature. Each sample was heated to the temperature range between T_g and T_x, and held at the desired temperature for 1 h. The appearance of the levitated sample changed from transparent to translucent at temperatures higher than 750 ºC. This was attributed to devitrification by crystallization. These results suggest that too much crystallization inhibits PL emission. The optimal heat treatment was 750 ºC for high efficiency PL emission. The refractive index and Abbe number of the transparent as-levitated Sm-BTS were measured to be 1.76 and 42, respectively. Because the Abbe number of transparent Sm-BTS glass represents high value more than 20, it is expected to be used utilized for optical devices.

Conclusions

Sm^{3+} doped $Ba_2TiSi_2O_8$ (BTS) glasses were prepared by aerodynamic levitation. The effects of the heat-treatment temperature on the crystallization behavior were investigated.

1. The crystallization rate of the levitated Sm^{3+} doped BTS sample was slower than that of the conventional melt-quenched glass, showing enhanced glass stability

2. With increasing heat treatment temperature, the

lattice parameter, *a*, of crystalline BTS crystals formed in glass decreased but the lattice parameter, *c*, of that increased. This result was attributed to the crystallization-induced stress formed in the crystallization process.

3. The values of the Avrami exponent (n) calculated using the Ozawa equation was approximately 3, which means that volume crystallization predominated in levitated Sm^{3+}-doped BTS glass during crystallization. The activation energies using the modified Ozawa equation and modified Kissinger equation were calculated to be 530.3 kJ/mol and 524.3 kJ/mol, respectively.

4. Nanocrystallized Sm^{3+} doped BTS glass exhibited yellow-green (564 nm), orange (601 nm) and red (647 and 709 nm) luminescence. The optimal heat treatment was found to be 750 ºC for high efficiency PL emission. The refractive index and Abbe number of the transparent as-levitated Sm-BTS were measured to be 1.76 and 42, respectively.

Acknowledgments

This study was supported by the National Research Foundation of Korea funded by the Ministry of Education, Science and Technology (NRF-2012 RIAIA2008361) and INHA UNIVERSITY Research Grant.

References

1. G. H. Beall, and L. R. Pinckney, J. Am. Ceram. Soc. 82 (1999) 5-16.
2. R. Sakai, Y. Benino, and T. Komatsu, Appl. Phys. Lett. 77 (2000) 2118-2120.
3. F. Torres, K. Narita, Y. Benino, T. Fujiwara, and T. Komatsu, J. Appl. Phys. 94 (2003) 5265-5272.
4. S. Prasad, K.B.R. Varma, Y. Takahashi, Y. Benino, T. Fujiwara, and T. Komatsu, J. Solid State Chem. 173 (2003) 209-215.
5. Y. Takahashi, K. Kitamura, Y. Benino, T. Fujiwara, and T. Komatsu, Appl. Phys. Lett. 86 (2005) 091110-1-091110-3.
6. N. Iwafuchi, S. Mizuno, Y. Benino, T. Fujiwara, T. Komatsu, M. Koide, and K. Matusita, Adv. Mater. Res. 11-12 (2006) 209-212.
7. S. Mizuno, Y. Benino, T. Fujiwara, and T. Komatsu, Jpn. J. Appl. Phys. 45 (2006) 6121-6125.
8. G. Blasse, J. Inor. Nucl.Chem. 30, 8 (1968) 2283-2284.
9. P.S. Bechthold, S. Haussuehl, E. Michael, J. Eckstein, K.Recker, and F. Wallrafen, Phys. Lett. A, 65 (1978) 453-454.
10. B. Zhu, S. Zhang, G. Lin, S. Zhou, and J. Oiu, J. Phys. Chem. C, 111 (2007) 17118-17121.
11. Y. Zhang, R. Pang, C. Li, C. Zang, Q. Su, J. Rare Earths, 28 (2010) 705-708.
12. Cabral, A. A., Fokin, V. M., Zanotto, E. D. and Chinaglia, C.R., J. Non-Cryst. Solids, 330 (2003) 174-186.
13. K. J. Lee, C. H. Lee, G. W. Lee, W. S. Hwang, C. H. Lee, S. Yoda, W. S. Cho, Thermochimica Acta, 542 (2012) 37-41.
14. K. J. Lee, M. S. V. Kumar, S. K. Jung, J. H. Jeong, C. H. Lee, M. W. Cho, G. W. Lee, C. H. Lee, S. Yoda, and W. S. Cho, J. Ceram. Process. Res. 14 (2013) 311-314.
15. J. Yu, N. Koshikawa, Y. Arai, S. Yoda, and H. Saitou, J. Cryst. Growth, 231 (2001) 568-576.
16. A. S. Gandhi, A. Saravanan, and V. Jayaram, Mater. Sci. Eng. A221 (1996) 68-75.
17. M. Erol, S. Kucukbayrak, A. Ersoy-Mericboyu, J. Non-Cryst. Solids, 355 (2009) 569-576.
18. S. K. Jung, Phd. Thesis, Inha university (2015) 52-53.
19. J. B. Nelson, and D. P. Riley, Proc. Phys. Soc. 57 (1945) 160-177.
20. A. Hrubý, Czech. J. Phys. B 22 (1972) 1187-1193.
21. E. A. Brandes, and G. B. Brook, Smithells Metals Reference Book 7th edition, Butterworth-Heinemann Ltd (1992).
22. Y. Ochi, Mater. Res. Bull. 41 (2006) 740-750.
23. T. Ozawa, Polymer, 12 (1971) 150-158.
24. M. Çelikbilek, A. E. Ersundu, N. Solak, S. Aydin, J. Non-Cryst. Solids, 357 (2011) 88-95.
25. K. Matusita, and S. Sakka, Bull. inst. chem. res. 59 (1981) 159-171.
26. B. Rangarajan, T. Shrout, and M. Lanagan, J. Am. Ceram. Soc. 92 [11] (2009) 2642-2647.